

Dynamics of path aggregation in the presence of turnover

DEBASISH CHAUDHURI¹, PETER BOROWSKI², P. K. MOHANTY³ and MARTIN ZAPOTOCKY^{1,4}

¹ *Max Planck Institute for the Physics of Complex Systems, Nöthnitzer Strasse 38, 01187 Dresden, Germany*

² *Department of Mathematics, University of British Columbia, Vancouver, BC, Canada V6T 1Z2*

³ *TCMP Division, Saha Institute of Nuclear Physics, 1/AF Bidhan Nagar, Kolkata 700064, India*

⁴ *Institute of Physiology, Academy of Sciences of the Czech Republic, Videnska 1083, 14220 Praha 4, Czech Republic*

PACS 05.40.-a – Fluctuation phenomena, random processes, noise, and Brownian motion

PACS 05.40.Fb – Random walks and Levy flights

PACS 87.19.1x – Development and growth

Abstract. - We investigate the slow time scales that arise from aging of the paths during the process of path aggregation. This is studied using Monte-Carlo simulations of a model aiming to describe the formation of fascicles of axons mediated by contact axon-axon interactions. The growing axons are represented as interacting directed random walks in two spatial dimensions. To mimic axonal turnover, random walkers are injected and whole paths of individual walkers are removed at specified rates. We identify several distinct time scales that emerge from the system dynamics and can exceed the average axonal lifetime by orders of magnitude. In the dynamical steady state, the position-dependent distribution of fascicle sizes obeys a scaling law. We discuss our findings in terms of an analytically tractable, effective model of fascicle dynamics.

Introduction. – The process of path aggregation is a ubiquitous phenomenon in nature. Some examples of such phenomena are river basin formation [1], aggregation of trails of liquid droplets moving down a window pane, formation of insect pheromone trails [2–4], and of pedestrian trail systems [5, 6].

Path aggregation has been mathematically studied mainly in two classes of models. One of them is known as the active-walker models [6] in which each walker in course of its passage through the system changes the surrounding environment locally, which in turn influences the later walkers. An example of such a process is the ant trail formation [2, 3]. While walking, an ant leaves a chemical trail of pheromones which other ants can sense and follow. The mechanism of human and animal trail formations is mediated by the deformation of vegetation that generates an interaction between earlier and later walkers [6]. A mathematical formalism to study the formation of such trails has been developed in Ref. [5, 6]. The other class of models showing path aggregation deals with non-interacting random walkers moving through a fluctuating environment. In Ref. [7], condensation of trails of particles moving in an environment with Gaussian spatial and temporal correlation is demonstrated analytically. Another example of this model class is the Scheidegger river model [1] (and related models [8]) which describes the formation of a stream net-

work by aggregation of streams flowing downhill on a slope with local random elevations.

In this Letter we analyze the dynamics of path aggregation using a simple model that belongs to the class of active walker systems discussed above. The model is similar to the one used to study path localization in Ref. [9]. In our model, however, we take into account the aging of the paths, an important aspect of the active walker models. For instance, in ant trail systems, the pheromone trails age due to evaporation. In the mammalian trail formation the deformations of the vegetation due to the movement of a mammal decays continuously with time [6]. In our model, the individual paths do not age gradually, but rather maintain their full identity until they are abruptly removed from the system. This particular rule for path aging is chosen to allow application of our model to the process of axon fasciculation, which we discuss next.

During the development of an organism, neurons located at peripheral tissues (e.g. the retina or the olfactory epithelium) establish connections to the brain via growing axons. The *growth cone* structure at the tip of the axon interacts with other axons or external chemical signals and can bias the direction of growth when spatially distributed chemical signals are present [10]. In the absence of directional signals, the growth cone maintains an approximately constant average growth direction, while

exploring stochastically the environment in the transverse direction [11]. The interaction of growth cones with the shafts of other axons commonly leads to fasciculation of axon shafts [12]. During development a significant portion of fully grown neurons die and get replaced by newborn neurons with newly growing axons. For certain types of neurons (such as the sensory neurons of the mammalian olfactory system) the turnover persists throughout the lifespan of an animal. In mice, the average lifetime of an olfactory sensory neuron is 1–2 months [13], which is less than one tenth of the mouse lifespan. The mature connectivity pattern is fully established only after several turnover periods [14].

The model we propose in this Letter captures the basic ingredients of the process of axon fasciculation, i.e. attractive interaction of growth cones with axon shafts, as well as neuronal turnover. The main contribution of this Letter is a detailed discussion of the slow time scales that emerge from the dynamics of our model. Using Monte-Carlo simulations we characterize the time scale for the approach to steady state and the correlation time within the steady state, and show that they can exceed the average axonal life time by orders of magnitude. To understand these results we formulate an analytically tractable effective single fascicle dynamics. This allows us to relate the observed slow time scales to the dynamics of the basins of the fascicles. From the effective fascicle dynamics we derive three time scales which we compare to the time scales extracted from the Monte-Carlo simulation of the full system.

For clarity, we stress that the dynamics of our model differs substantially from one-dimensional coalescence ($A + A \rightarrow A$) [15] or aggregation ($mA + nA \rightarrow (m+n)A$) [16]. In our model, there is no direct inter-walker interaction; rather, each random walker interacts locally with the *trails* of other walkers. While the stationary properties of the system (such as the fascicle size distribution in the steady state) may be approximately understood using an analogy to one-dimensional diffusion with aggregation, the dynamical properties (such as the time scale of approach to the steady state, and the correlation time in the steady state) are undefined in the one dimensional analogy, and require understanding based on the full two dimensional model. This is in contrast to the situation for path aggregation models without turnover: e.g., the Scheidegger river network model can be mapped onto the Takayasu model of diffusion-aggregation in presence of injection of mass in one dimension [17].

Model and numerical implementation. – Each growing axon is represented as a directed random walk in two spatial dimensions (Fig. 1a). The random walkers (representing the growth cones) are initiated at the periphery ($y = 0$, random x) with a birth rate α , and move towards the target area (large y) with constant velocity $v_y = 1$. In the numerical implementation on a tilted square lattice, at each time step the growth cone at (x, y) can move to $(x - 1, y + 1)$ (left) or $(x + 1, y + 1)$ (right).

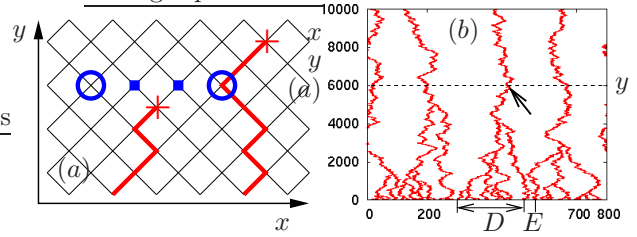


Fig. 1: (Color online) (a) Interacting directed random walks on a tilted square lattice. A random walker (+) represents a growth cone. For one walker, the possible future sites (\square) and their nearest neighbours (\circ) are marked. The trail of a walker (line) models an axon shaft. (b) Typical late-time configuration ($t = 25T$) in a system with $L = 800$ and $N_0 = 100$. For the fascicle identified at $y = 6000$ (arrow), D indicates its basin, i.e. the interval at the level $y = 0$ between the right-most and left-most axons belonging to the fascicle. The gap E is the inter-basin free space at $y = 0$. Note that the y -coordinate cannot be understood as equivalent to time (see the main text).

(Note that the sites are labeled alternatively by even x and odd x at successive y levels.) The probability $p_{\{L,R\}}$ to move left/right is evaluated based on the axon occupancy at the $(x - 1, y + 1)$ and $(x + 1, y + 1)$ sites and their nearest neighbours (see Fig. 1a). In the simplest version of the model, the interaction is governed by the “always attach, never detach” rule: $p_L = 1$ when among the sites $(x \pm 1, y + 1)$, $(x \pm 3, y + 1)$ only $(x - 3, y + 1)$ is already occupied; $p_R = 1$ when only $(x + 3, y + 1)$ is occupied; $p_L = p_R = 1/2$ in all other cases. Periodic boundary conditions are used in the x -direction.

To capture the effect of neuronal turnover, each random walker is assigned a lifetime from an exponential distribution with mean T . When the lifetime expires, the random walker and its entire trail is removed from the system. The mean number of axons in the system therefore reaches the steady state value $N = N_0 \exp(-\beta y)$ where $N_0 = \alpha/\beta$, and $\beta = 1/T$ is the death rate per axon. In the simulations, we use $T = 10^5$ time steps, and restrict our attention to $y \leq T/10$. The birth rate α is chosen so as to obtain the desired number of axons N_0 , or equivalently, the desired axon density $\rho = N_0/L$ ($\rho = 1/2$ implies an average occupancy of one axon per site), where L is the system size in x -direction. The presence of turnover distinguishes our model from previous theoretical works on axon fasciculation [18, 19]. The y -coordinate in Fig.1a cannot be viewed as equivalent to time, and the dynamics at fixed y (which is the main focus of this Letter) has no analogy in one dimensional models of aggregation or coalescence.

Mean fascicle size: A typical late-time configuration for a system with $L = 800$ and $N_0 = 100$ is shown in Fig. 1b. With increasing fasciculation distance y , the axons aggregate into a decreasing number $m(y)$ of *fascicles*. (At a given y , two axons are considered to be part of the same fascicle if they are not separated by any unoccupied sites.) The number of axons in the fascicle is referred to as the fascicle size n . The mean fascicle size \bar{n} at level y may be

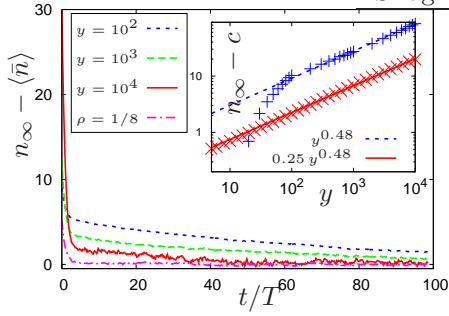


Fig. 2: (Color online) Approach to the steady state in the $L = 400, N_0 = 200$ system at representative y -levels indicated in the legend. The mean fascicle size $\langle \bar{n}(t; y) \rangle$ [averaged over 10^3 initial conditions] approaches $n_\infty(y)$ as $t \rightarrow \infty$. The data set labeled as $\rho = 1/8$ is from the $L = 400, N_0 = 50$ system, collected at $y = 5000$. Inset: Power-law growth of mean fascicle size $n_\infty - c = 2\rho y^b$ in the steady state. The values of the growth exponent and offset are: $b = 0.48, c = 1.3$ for the $L = 800, N_0 = 100$ system(\times), and $b = 0.48, c = 6.9$ for the $L = 400, N_0 = 200$ system($+$).

estimated using the following mean-field argument. Each of the m fascicles collects axons that were initiated on an interval of length $D \simeq L/m = L\bar{n}/N$ at the level $y = 0$ (see Fig. 1b). The axons initiated at opposite edges of the interval are expected to meet within $y \simeq (D/2)^2$ steps of the random walk in x -direction. Consequently, $\bar{n} \simeq DN/L \simeq 2\rho y^{1/2} \exp(-\beta y)$ for y up to $y \simeq (L/2)^2$, where complete fasciculation ($\bar{n} = N$) is expected. Thus for $y \ll (L/2)^2$ and $\beta y \ll 1$ (which are satisfied in our simulations) one obtains the power law growth $\bar{n} \simeq 2\rho y^{1/2}$.

Slow time scales. – The measured mean fascicle size, obtained by averaging over all the existing fascicles at a given y (Fig. 2), grows with time as $\bar{n} = n_\infty - p \exp(-\beta t) - q \exp(-t/\tau_{ap})$, where $\tau_{ap}(y)$ defines the time scale of approach to the steady state value $n_\infty(y)$. We find that τ_{ap} is an increasing function of y (up to $y \simeq (L/2)^2$ where a single fascicle remains and τ_{ap} drops to T), and can exceed the axon lifetime T by orders of magnitude (Figs. 2 and 3b). Asymptotically in y , we find $n_\infty = c + 2\rho y^b$, with $b = 0.480 \pm 0.018$ (Fig. 2 inset) – in reasonable agreement with the mean-field prediction.

The dynamics in the steady state is characterized by the auto-correlation function for the mean fascicle size $\bar{n}(t)$ at a fixed y -level: $c(t) = \langle \bar{n}(t)\bar{n}(0) \rangle$ which fits to the form $p + q \exp(-\beta t) + r \exp(-t/\tau_c)$. In Fig. 3a we plot the subtracted correlation function $g(t) = [c(t) - p]/(q + r)$. The correlation time τ_c increases with y and significantly exceeds the axon lifetime T (Fig. 3b).

Effective fascicle dynamics at fixed y . – We next examine the dynamics of individual fascicles. These are typically long lived, but at a given y -level the fascicles very rarely merge or split (data not shown). Consequently, the number $n(t)$ of axons in each fascicle may be viewed

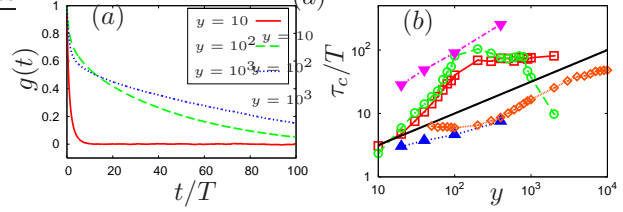


Fig. 3: (Color online) (a) Subtracted auto-correlation $g(t)$ at y -levels indicated in the legend for the $L = 100, N_0 = 50$ system. The time series $\bar{n}(t)$ is collected over $t = 200T$ to $2 \times 10^4 T$; $g(t)$ is further averaged over 30 initial conditions. (b) The correlation time τ_c (\square) and approach-to-steady-state time scale τ_{ap} (\circ) as a function of y . The theoretical time-scales τ (filled \triangle), τ_f (filled ∇) (see text) are evaluated from the values of a_+, b_+, c_+ in Table I. The solid line is y^b with $b = 1/2$. τ_c (\diamond) for the $L = 400, N_0 = 50$ system is also shown.

as given by a stochastic process specified by the rates $u_\pm(n, y)$ (for transitions $n \rightarrow n \pm 1$). At fixed y , a fascicle can loose an axon only when the axon dies, thus $u_-(n) = \beta n$, independent of y .

The gain rate $u_+(n, y)$ is governed by the properties of the fascicle *basin* (see Fig. 1b). Under the “always attach, never detach” rule, new axons initiated anywhere within the basin of size D cannot escape the fascicle. In addition, some of the axons born in the two gaps (of size E) flanking the basin contribute. Therefore,

$$u_+ = \alpha D/L + (\alpha E/L)[1 - \Pi(E, y)] \quad (1)$$

where $\Pi(E, y)$ is the probability that an axon born within the gap of size E survives as a single axon at level y .

The two stochastic variables that fully characterize the dynamics of a fascicle are the number of axons $n(t)$ and the basin size $D(t)$. In Fig. 4a, we plot $n(t)$ and $D(t)$ for a specific fascicle followed over $200T$. It is seen that n and D tend to co-vary (cross correlation coefficient $c(D, n) = 0.74$). In the following we treat the dynamics of D as slave to the dynamics of n , i.e. we assume that the average separation $S = D/(n - 1)$ between two neighbouring axons within the basin is time-independent. This implies $u_+(n) = a + bn$ with $b = \beta \rho S$.

The measured average gain rate $u_+(n)$ in the steady state [20] deviates from linearity at high n , but is well fit by $u_+(n) = a_+ + b_+ n - c_+ n^2$ (Fig. 4b). The quadratic correction may be understood as a saturation effect which reflects that basins of size D can not exceed $2y$ or L and $D > 2y^{1/2}$ occur with low probability. The quadratic correction to the linear growth of u_+ with n becomes significant at $n \gtrsim 2y^{1/2} \rho \approx \bar{n}$. Note that the coefficients a_+, b_+ and c_+ are functions of y .

Master equation at fixed y : Let $P(n, t)$ be the distribution of fascicles of size n at time t at a fasciculation distance y . The master equation of the effective birth-death

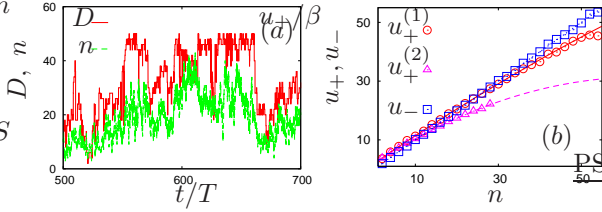


Fig. 4: (Color online) (a) Time series of number of axons n and basin size D for an individual fascicle in a system of $L = 100$ and $N_0 = 50$ at $y = 400$. The equal time cross correlation coefficient averaged over this time-span, $c(D, n) = [\langle Dn \rangle - \langle D \rangle \langle n \rangle] / \sqrt{[\langle D^2 \rangle - \langle D \rangle^2][\langle n^2 \rangle - \langle n \rangle^2]} = 0.74$. (b) Mean gain and loss rates (in units of β) [averaged over 10^3 initial conditions and the interval $100T \leq t \leq 150T$] as a function of fascicle size n . The rates are measured at $y = 400$ in a system with $L = 100$. The fits (lines) are $u_- = n$, $u_+^{(1)} = 1.92 + 0.974n - 0.002n^2$ (for $N_0 = 50$), and $u_+^{(2)} = 1.95 + 0.927n - 0.008n^2$ (for $N_0 = 25$).

process may be written as

$$\begin{aligned} \dot{P}(n, t) &= u_+(n-1)P(n-1, t) + u_-(n+1)P(n+1, t) \\ &- [u_+(n) + u_-(n)]P(n, t), \end{aligned} \quad (2)$$

for $n > 1$. For the boundary state ($n = 1$)

$$\dot{P}(1, t) = J_+(y) + u_-(2)P(2, t) - [u_+(1) + u_-(1)]P(1, t)$$

where $J_+(y)$ represents the rate with which new single axons appear between existing fascicles at y . In the steady state, $J_+(y)$ is balanced by the rate with which existing fascicles disappear from the system, i.e. $J_+(y) = u_-(1)P_s(1)$. The steady state condition $\dot{P}(n, t) = 0$ then implies pairwise balance, $u_+(n-1)P_s(n-1) = u_-(n)P_s(n)$, for all $n > 1$. Thus the steady state distribution is given by $P_s(n) = J_+(y) \frac{1}{u_-(n)} \prod_{k=1}^{n-1} \frac{u_+(k)}{u_-(k)}$, with the normalization condition $\sum_{n=1}^{\infty} nP_s(n, y) = N$. In order to obtain a closed-form expression for $P_s(n, y)$, we expand the pairwise balance condition up to linear order in $1/N$ and solve to find,

$$\beta P_s(n, y) \simeq J_+(y) n^\gamma \exp[-\ell(n-1) - \kappa(n-1)^2], \quad (3)$$

where $\gamma = a_+/\beta - 1$, $\ell = 1 - b_+/\beta$ and $\kappa = c_+/2\beta$.

Time scales: Three distinct time scales may be extracted from the effective birth-death process. The correlation time τ for the fascicle size n , near the macroscopic stationary point n_s [$u_+(n_s) = u_-(n_s)$] can be expressed [21] as $\tau = 1/(u'_-(n_s) - u'_+(n_s)) = 1/(\beta - b_+ + 2c_+n_s)$. With a linear approximation of $u_+(n) = a_+ + b_+n$ the approach-to-steady-state time scale for $\langle n \rangle$ is $\tau_{ap} = 1/(\beta - b_+)$ [21]. We note that the long time scales do not simply arise as a consequence of fascicles containing many axons, but are due to the dynamics of the fascicle basins. To see that, imagine a fascicle with frozen boundary axons, for which $u_+ \approx (\alpha/L)D$ with D constant. In this case $u'_+(n_s) = 0$ and the correlation time $\tau \simeq T$. To obtain

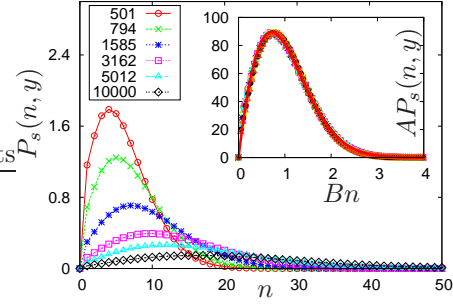


Fig. 5: (Color online) Steady state distribution of fascicle sizes $P_s(n, y)$ [averaged over 10^4 initial conditions and the time interval $10T \leq t \leq 25T$] for the $N_0 = 100$, $L = 800$ system at y -levels indicated in the legend. Inset: A scaling with $B = 1/\langle n \rangle$ and $A = \langle n \rangle^{2.1}$ collapses all data obtained for $y = 1585, 1995, 3162, 5012, 6310, 7943, 10^4$ onto a single curve $\phi(u) = \mathcal{N}u \exp(-\nu u - \lambda u^2)$ with $u = n/\langle n \rangle$ and $\mathcal{N} = 274$, $\nu = 0.78$, $\lambda = 0.45$.

$\tau > T$, D must co-vary with n . At high y , $u'_+ \approx 1/T$ resulting in $\tau \gg T$. We note that in the full system, the dynamics of the basin size can be viewed as arising from the competition between neighbouring fascicles for basin space.

A third time scale τ_f can be defined by $J_+(y) = m/\tau_f$, and reflects the rate of turnover of *fascicles* in the full system. Evaluating, $\tau_f = [\int_1^\infty P_s(n, y) dn] / J_+(y)$ using $P_s(n, y)$ from Eq. 3 (with $\gamma = 1$), we obtain

$$\tau_f = (T/2\kappa) \left[1 - \left(\sqrt{\pi} e^{\frac{\ell^2}{4\kappa}} (\ell - 2\kappa) \operatorname{erfc}(\ell/2\sqrt{\kappa}) \right) / 2\sqrt{\kappa} \right]. \quad (4)$$

Fascicle size distribution in the steady state. – Following the discussions on effective single fascicle dynamics, we now return to the simulation results for the dynamics of the whole system. The steady state is characterized by the stationary distribution of fascicle sizes $P_s(n, y)$, defined as the number of fascicles of size n at level y . For a system with $L = 800$ and $N_0 = 100$, $P_s(n, y)$ is shown at a series of y -levels in Fig. 5. Within the range $y = 10^3 - 10^4$ all data collapse onto a single curve after appropriate rescaling (Fig. 5). This data collapse implies the scaling law

$$P_s(n, y) = \langle n(y) \rangle^{-2.1} \phi(n/\langle n(y) \rangle) \quad (5)$$

where the scaling function $\phi(u) = \mathcal{N}u \exp(-\nu u - \lambda u^2)$.

Analogy to particle aggregation in one dimension. – As we have stressed in the introduction, the full dynamics of our system can not be mapped onto the particle dynamics of a one-dimensional reaction-diffusion system. At fixed time t (within the steady state), however, the aggregation of fascicles with increasing y may be formally viewed as the evolution of an irreversible aggregation process $mA + nA \rightarrow (m+n)A$ in one spatial dimension, where the y -coordinate (Fig.1(b)) takes the meaning

y	a_+/β	b_+/β	c_+/β	y	$\langle S \rangle$
20	1.96	0.862	0.0116	200	1.14
40	1.94	0.909	0.0082	400	1.60
100	1.96	0.947	0.0056	1000	2.02
400	1.92	0.974	0.0022	10000	2.21

Table 1: y -dependence of the fascicle parameters defined in the main text. System parameters are $L = 100$ and $N_0 = 50$.

of time. This exhibits analogous scaling properties, but with a different scaling function $u \exp(-\lambda u^2)$ [16], which lacks the exponential part $\exp(-\nu u)$. It is interesting to note at this point that to remove the exponential part in the expression of the steady state distribution (Eq.3) one would require $b_+ = \beta$ which in turn implies $\tau_{ap} = \infty$. In other words, without the exponential part $\exp(-\nu u)$ the emerging long time scale τ_{ap} is lost. This is consistent with the fact that the time scales arising from turnover are undefined in the one dimensional analogy.

Scaling of y -dependent parameters. – The expansion coefficients for $u_+(n, y)$, measured at selected y -levels in a system with $L = 100$ and $N_0 = 50$, are listed in Table I. The scaling property of the distribution of fascicle sizes (Eq. 5) implies $P_s(n, y) = \mathcal{N} y^{-3.1b} n \exp(-\nu n y^{-b} - \lambda n^2 y^{-2b})$. Consistency with Eq. 3 requires $J_+(y) \sim y^{-3.1b}$, $\kappa \sim y^{-2b}$ [i.e. $c_+ \sim y^{-2b}$], and $\ell \sim y^{-b}$ [i.e. $(\beta - b_+) \sim y^{-b}$]. This is in reasonable agreement with the data in Table I. The coefficient $a_+ \simeq 2\beta$ for all y reflects $\gamma \simeq 1$. Notice that $J_+(y) \propto \Pi(E, y)$ the probability that an axon born in the gap remains single at the level y . $\Pi(E, y)$ can be approximated as the survival probability of a random walker moving in between two absorbing boundaries (basin borders) each of which is undergoing random walk; thus $\Pi \sim y^{-3/2}$ [16]. This is consistent with the measured exponent in $J_+(y) \sim y^{-3.1b}$.

The gradual approach of $b_+ \approx \beta \rho S$ to β with increasing y may be understood as follows. At low y , fascicles are formed preferentially by axons that started with small separation S at the $y = 0$ level, and the typical gap size E exceeds S . With increasing y , the smallest gaps are removed to become part of fascicles; consequently both E and S grow with y , and S approaches $1/\rho$ at high y . The time averaged S for selected fascicles is shown in the last two columns of Table I.

y -dependence of time scales: The y -dependence of parameters discussed above implies the following scaling for the theoretically derived time scales: the approach-to-steady-state time $\tau_{ap} = 1/(\beta - b_+) \sim y^b$, the correlation time $\tau \sim \tau_{ap} \sim y^b$ and the life time of fascicles $\tau_f \sim 1/\kappa \sim y^{2b}$. As seen in Fig. 3b, the measured correlation time τ_c falls in between the computed time scales τ and τ_f , and the three time scales show distinct y -dependence. In a system with lower axon density, the time scales are reduced (Fig. 3b) as the increased inhomogeneity of axon separations at $y = 0$ leads to a stronger deviation of ρS from 1.

Conclusion. – To summarize, we have proposed a simple model for axon fasciculation that shows rich dynamical properties. We identified multiple time scales that grow with the fasciculation distance y and become $\gg T$, the average lifetime of individual axons. The slow time scales do not simply arise as a consequence of fascicles containing many axons, but are due to the dynamics of the fascicle basins. Our theoretical results have wider relevance for existing related models (e.g. of insect pheromone trails [2–4] and pedestrian trail formation [5, 6]), in which the slow maturation and turnover of the connectivity pattern have not been analyzed in detail.

To conclude, we comment on the applicability of our model to the biological system which we described in the introduction, i.e. the developing mammalian olfactory system. The model presented in this Letter is readily generalized to include multiple axon types, type-specific interactions, and detachment of axons from fascicles [22]. This is important as in the olfactory system the nasal epithelium contains neurons belonging to multiple types, distinguished by the expressed olfactory-receptor [12], with type specific interaction strengths [23]. (We note, however, that preparing transgenic mice expressing only a single olfactory-receptor has recently become a reality [24]). A further modification of the basic model that might be required is the introduction of history-dependent axonal lifetimes [25]. A comparatively simpler task is to relate our model to experimental studies of axon growth in neuronal cell culture [26, 27].

* * *

We gratefully acknowledge extensive discussions with Paul Feinstein on olfactory development and on the formulation of our model.

REFERENCES

- [1] A. E. Scheidegger, Int. Assoc. Sci. Hydrol. Bull. **12**, 15 (1967).
- [2] M. M. Millonas, J. Theor. Biol. **159**, 529 (1992).
- [3] J. Watmough and L. Edelstein-Keshet, J. Theor. Biol. **176**, 357 (1995).
- [4] F. Schweitzer, K. Lao, and F. Family, Biosystems **41**, 153 (1997).
- [5] D. Helbing, J. Keltsch, and P. Molnár, Nature **388**, 47 (1997).
- [6] D. Helbing, F. Schweitzer, and P. Molnár, Phys. Rev. E **56**, 2527 (1997).
- [7] M. Wilkinson and B. Mehlig, Phys. Rev. E **68**, 040101 (2003).
- [8] I. Rodrigues-Iturbe and A. Rinaldo, *Fractal river basins* (Cambridge University Press, Cambridge, UK, 2001).
- [9] B. M. Schulz, P. Reineker, and M. Schulz, Phys. Lett. A **299**, 337 (2002).
- [10] S. F. Gilbert, *Developmental Biology*, 8th ed. (Sinauer Associates Inc., Sunderland, MA, 2006), Chap. 3.
- [11] M. J. Katz, J. NeuroSci. **5**, 589 (1985).

- [12] P. Mombaerts, *Annu. Rev. Cell. Dev. Biol.* **22**, 713 (2006).
- [13] L. Crews and D. Hunter, *Persp. Dev. Neurobiol.* **2**, 151 (1994).
- [14] D.-J. Zou, P. Feinstein, A. L. Rivers, G. A. Mathews, A. Kim, C. A. Greer, P. Mombaerts, and S. Firestein, *Science* **304**, 1976 (2004).
- [15] D. ben Avraham, in *Nonequilibrium statistical mechanics in one dimension*, edited by V. Privman (Cambridge University Press, Cambridge, UK, 1997).
- [16] S. Redner, *A guide to first passage processes*, 3rd ed. (Cambridge University Press, Cambridge, UK, 2001).
- [17] M. Takayasu and H. Takayasu, in *Nonequilibrium statistical mechanics in one dimension*, edited by V. Privman (Cambridge University Press, Cambridge, UK, 1997).
- [18] H. G. E. Hentschel and A. V. Ooyen, *Physica A* **288**, 369 (2000).
- [19] J. K. Krottje and A. V. Ooyen, *Bulletin of Mathematical Biology* **69**, 3 (2007).
- [20] At a given y -level, we count the axon arrivals and deaths during an extended time period, and record the size of the fascicle that was affected in each event. By definition, per unit time $u_+(n, y)P(n, y)$ fascicles of size n gain an axon, while $u_-(n, y)P(n, y)$ fascicles of size n lose an axon.
- [21] V. Kampen, *Stochastic processes in physics and chemistry*, 2nd ed. (North Holland Publishing Limited, Amsterdam, 1992).
- [22] D. Chaudhuri, P. Borowski, and M. Zapotocky (unpublished).
- [23] A. Vassalli, A. Rothman, P. Feinstein, M. Zapotocky, and P. Mombaerts, *Neuron* **35**, 681 (2002).
- [24] T. Imai, M. Suzuki, and H. Sakano, *Science* **314**, 657 (2006).
- [25] Paul Feinstein, private communication.
- [26] M. G. Honig, G. G. Petersen, U. S. Rutishauser, and S. J. Camilli, *Dev. Biol.* **204**, 317 (1998).
- [27] J. A. Hamlin, H. Fang, and J. E. Schwob, *J. Comp. Neuro.* **474**, 438 (2004).